Effect of Tether Conductivity on the Efficiency of Photoisomerization of Azobenzene-Functionalized Molecules on Au{111}

ARTICLE *in* JOURNAL OF PHYSICAL CHEMISTRY LETTERS · SEPTEMBER 2012

Impact Factor: 7.46 · DOI: 10.1021/jz300968m

9 AUTHORS, INCLUDING:

Bala Krishna Pathem
HGST, A Western Digital Company
12 PUBLICATIONS **187** CITATIONS
SEE PROFILE

Yuebing Zheng
University of Texas at Austin
65 PUBLICATIONS **1,513** CITATIONS
SEE PROFILE

John L Payton
Youngstown State University
16 PUBLICATIONS **196** CITATIONS
SEE PROFILE

Paul S Weiss
University of California, Los Angeles
395 PUBLICATIONS **11,932** CITATIONS
SEE PROFILE

THE JOURNAL OF PHYSICAL CHEMISTRY Letters

Letter

pubs.acs.org/JPCL

Effect of Tether Conductivity on the Efficiency of Photoisomerization of Azobenzene-Functionalized Molecules on Au{111}

Bala Krishna Pathem,[†,‡] Yue Bing Zheng,[†,‡,§] John L. Payton,[∥] Tze-Bin Song,[†,§] Byung-Chan Yu,[⊥] James M. Tour,[⊥] Yang Yang,*[,†,§] Lasse Jensen,*[,∥] and Paul S. Weiss*[,†,‡,§]

[†]California NanoSystems Institute, [‡]Department of Chemistry & Biochemistry, and [§]Department of Materials Science & Engineering, University of California, Los Angeles, Los Angeles, California 90095, United States

[∥]Department of Chemistry, The Pennsylvania State University, University Park, Pennsylvania 16802, United States

[⊥]Department of Chemistry and The Smalley Institute for Nanoscale Science and Technology, Rice University, Houston, Texas 77005, United States

Supporting Information

ABSTRACT: We establish the role of tether conductivity on the photoisomerization of azobenzene-functionalized molecules assembled as isolated single molecules in well-defined decanethiolate self-assembled monolayer matrices on Au{111}. We designed the molecules so as to tune the conductivity of the tethers that separate the functional moiety from the underlying Au substrate. By employing surface-enhanced Raman spectroscopy, time-course measurements of surfaces assembled with azobenzene functionalized with different tether conductivities were independently studied under constant UV light illumination. The decay constants from the analyses reveal that photoisomerization on the Au{111} surface is reduced when the conductivity of the tether is increased. Experimental results are compared with density functional theory calculations performed on single molecules attached to Au clusters.

SECTION: Physical Processes in Nanomaterials and Nanostructures

Precise control over the reversible isomerization of functional molecules when assembled on solid surfaces is of great importance to understand the rules of molecular- and supramolecular-scale action.[1−14] Various kinds of photochromic molecules such as azobenzene,[15−24] diarylethene,[9,25−27] spiropyran,[28−30] and more recently dihydroazulene[31−34] have been investigated as possible candidates for molecular switches. These families of functional molecules have relative advantages and disadvantages due to factors such as their ease of molecular assembly on substrates, quantum yield of photoisomerization, reversibility of isomerization, and quenching of isomerization by the underlying substrate. Of these families of photochromic molecules, azobenzenes have thus far attracted the greatest attention.

Azobenzene (henceforth **Azo**) exists in a near-planar trans conformation in its thermodynamically stable state with nearly zero dipole moment.[35,36] When irradiated with UV light at ∼365 nm, the molecule isomerizes to a nonplanar cis conformation via rotation of a phenyl group out of the plane of the azobenzene moiety, carrying a dipole moment of 3 D.[36] Upon subsequent irradiation with ∼420 nm visible light, the cis conformation reverts back to its original trans conformation, although thermal relaxation from cis to trans has also been shown to be a common pathway for the reverse reaction where relaxation times typically depend on the substituents on the azobenzene moiety ranging from minutes (for alkyl-substituted molecules) to days (for unsubstituted azobenzenes). Because of their difference in planarity, it has been established that trans form is approximately 100 times more conductive than cis,[16] and hence azobenzenes are considered to be a type of molecular switches.[22] Various theoretical and experimental studies have been performed to understand the mechanisms of photoisomerization of azobenezenes in the gas phase, in various solvents, and on solid substrates when isolated as single molecules or in ensembles. For instance, it has been well-established that photoisomerization of molecules such as azobenzene is quenched when the molecules are adsorbed directly on conductive substrates such as Au{111}.[20] However, by attaching a relatively nonconductive tether to the azobenzene functional moiety, the molecules can be spatially separated from the substrate, and a dramatic increase in the photoisomerization yield has been observed both at ensemble[37] and single-molecule scales.[22,38−40] Recently, surface-enhanced Raman spectroscopy (SERS) has been shown to be an excellent tool for following photoisomerization of functional molecules on the ensemble scale.[14,37,41]

Although, the effects of the surrounding environment,[42,43] the coupling of the functional moiety to the substrate using a

Received: July 16, 2012
Accepted: August 13, 2012

   dx.doi.org/10.1021/jz300968m | J. Phys. Chem. Lett. 2012, 3, 2388−2394

tether,[12,18,20−22,44,45] the conductivity of the substrate,[21,39,46] the length and free volume of the tether,[47,48] the structure of the substrate,[37,48−50] and ways to circumvent steric interactions between the azobenzene moieties[22,23,51,52] have been reported previously, the effects of the conductivity of the tethers on photoisomerization have not been reported. To employ such molecular switches in a range of conditions and chemical environments, it is imperative to understand the roles of all the key aspects constituting the photoswitches and their supporting structures. To that end, we investigate the role of the conductivity of the tether on the photoisomerization of azobenzene molecules when assembled on Au{111}.

We designed tethers to functionalize azobenzene molecules so that they could be covalently bound to Au substrates and such that the functional moiety is spatially separated from the conductive substrate to avoid direct surface quenching. We assembled these functional molecules as isolated single molecules by a coadsorption technique that we have previously reported.[22] This technique enables us to separate azobenzene-functionalized molecules from each other such that steric hindrance between neighboring molecules is precluded. We employed azobenzene functionalized with two kinds of tethers in this study: a less conductive, saturated linear alkyl chain tether (henceforth **Azo1**) and a more conductive, phenylene ethynylene tether (henceforth **Azo2**) (Figure 1). We used

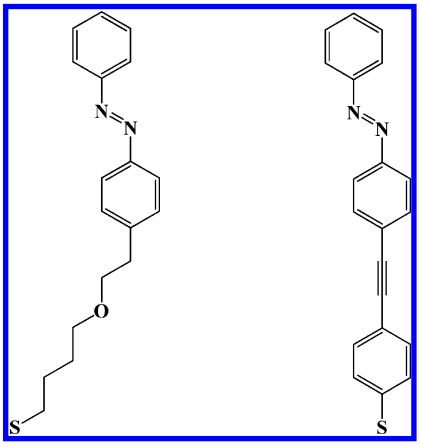

Figure 1. Schematic of (left) **Azo1** and (right) **Azo2**. Because of the linear alkyl chain, **Azo1** assumes ∼30° tilt with respect to surface normal, whereas **Azo2** assumes a nominally perpendicular orientation with respect to the Au{111} surface. (See Figure S2 of the Supporting Information.)

SERS to perform the time-course measurements of photoisomerization of these azobenzene-functionalized molecules on Au{111} in sufficient numbers to have significant statistics.[37,43,53,54]

The phenylene ethynylene tether in **Azo2** is expected to be substantially more conductive than the alkyl tether in **Azo1**. If the conductance of a molecule is given by $G = Ae^{-(\beta n)}$ (where A is constant and n is the length of the molecule), then the term β is a measure of molecular conductivity versus length. A number of studies have found that for saturated chains on Au $\beta \approx 1.0 \pm 0.1$ Å^{-1},[55−63] whereas for phenylene ethynylene molecules, with mixed sp and sp^2 hybridization, it is approximately a factor of 2 lower and $\beta \approx 0.57 \pm 0.02$ Å^{-1}.[64,65] Note that phenylene vinylene and other all sp^2-hybridized systems have β values another factor of two lower[66] and thus are more conductive (and would be expected to quench even faster than the tether in **Azo2**).

We have recently reported an efficient way to follow the photoisomerization using SERS.[37] Using this method, Au substrates with regular nanohole arrays were shown to enhance the signals of azobenzene Raman vibrational modes. Here we employed the same technique to follow the time-course measurements of both **Azo1** and **Azo2** molecules. Focused ion beam (FIB) lithography (Nova 600 NanoLab, FEI Company, Hillsboro, OR) was used to fabricate cylindrical nanoholes (with a diameter of 175 nm) in square arrays (with a period of 300 nm) into Au thin films.

The samples were prepared in the dark by immersing the flame-annealed Au{111} nanohole array substrates in a 1:4 mixture of ethanolic solutions of **Azo1** or **Azo2** and decanethiol (**C10**) (such that the final concentration of the solutions was 1 mM) for 24 h under a nitrogen atmosphere. The samples were then vapor-annealed over **C10** solutions at 80 °C for 2 h to backfill the **C10** matrix molecules.[67] This process, in which the substrate is heated and held over a neat liquid of **C10** molecules to be ordered, resulted in tight packing of the monolayer, thus hindering the surface mobility of the switch molecules.[43,56,68,69] The samples were then stored in the dark until further analysis.

A Renishaw inVia Raman system (Renishaw, IL) operating under ambient conditions was employed for Raman analysis. We chose a 632.8 nm He−Ne laser as the Raman excitation source considering the resonant wavelength of the Au substrates. Laser power and beam diameter were ∼17 mW and ∼1 μm, respectively. Each measurement was a convolution of 50 sweeps in the wavelength range of interest with a set integration time of 150 s. Wire 3.2 (Renishaw) and OriginPro software were used to analyze peak areas and to curve fit and to calculate decay constants, respectively.

To compare the experimental results with theory, we performed simulations to predict the Raman spectra of the trans and cis isomers of **Azo2** molecules attached to a Au_3 cluster. All calculation used the NWCHEM software package.[70] The B3LYP hybrid functional with the 6-31G* basis set for N, C, S, and H atoms and the LANL2DZ effective core potential for Au atoms were employed for all calculations of the geometric structure and vibrational frequencies. Vibrational frequencies were scaled by 0.9614; no imaginary frequencies were found. The Raman differential cross sections were calculated with a three-point numerical differentiation of the analytical polarizabilities with LC-ωPBE functional (ω = 0.3 Bohr^{-1}, α = 0.0, and β = 1.0) and the same basis set. The Raman differential cross sections were broadened with a Lorentzian having a full width at half-maximum of 20 cm^{-1} and an incident light of 514.5 nm. Raman signals for different mole fractions of the molecules were also calculated to gain a better understanding of the switching efficiencies of molecules on the substrate. The analogous calculations for **Azo1** (without the Au cluster) have been previously reported[37] and are used here in elucidating the role of the tether.

Figure 2 shows the overlay of simulated Raman spectra of **Azo2** molecules attached to Au_3 clusters as a convolution of various mole fractions of trans and cis isomers. The spectra have been offset for clarity. Multiple peaks in the range of 1000 to 1700 cm^{-1} were observed with major peaks at 1055, 1116, 1435, 1458, 1495, and 1573 cm^{-1} (see Figure S1 of the Supporting Information for schematics of all of these modes in trans and cis conformations). After considering all of the peaks in the simulated spectra, the peaks labeled P1 (1055 cm^{-1}) and

dx.doi.org/10.1021/jz300968m | J. Phys. Chem. Lett. 2012, 3, 2388−2394

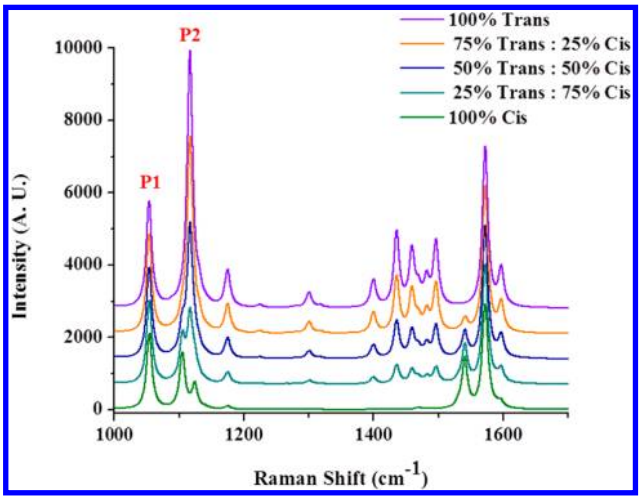

Figure 2. Simulation of trans and cis **Azo2** at various mole fractions as shown in the legend. The peaks labeled P1 and P2 were used to follow the kinetics of photoisomerization. The spectra have been offset for clarity.

P2 (1116 cm^{-1}) were identified as strong indicators of photoisomerization. Also, the area of the peak at 1540 cm^{-1} was observed to increase with trans−cis isomerization. This peak arises due to the vibration mode of the N═N double bond (Figure S1 of the Supporting Information) and is not prominent when the molecules are in the trans conformation; only when the molecule isomerizes does this vibrational mode become Raman active. Although we identified this peak in our experiments, the peak area was usually at or below the detection limit, and thus it was not used for quantitative measurements. Whereas all other peaks decrease in area, the areas of peaks at 1055 (P1) and 1573 cm^{-1} show very little change.

The Raman intensity usually scales with the polarizability of a system (because the Raman intensity derives from the polarizability derivatives $(\partial\alpha/\partial Q)^2$). Because the trans isomer (highly conjugated) is more polarizable, it is expected to have a stronger Raman signal than the less polarizable cis isomer (less conjugated), as observed in Figures 2 and 4. To explain the behavior of the P1 mode, we observe that the mode is mainly isolated to the tether ring, whereas P2 is mainly a ring breathing mode of the azobenzene unit (Figure 3). The trans-to-cis isomerization reduces the conjugation and thus the polarizability of the azobenzene unit but not that of the tether, at least not directly. Therefore, it is not surprising to find that the

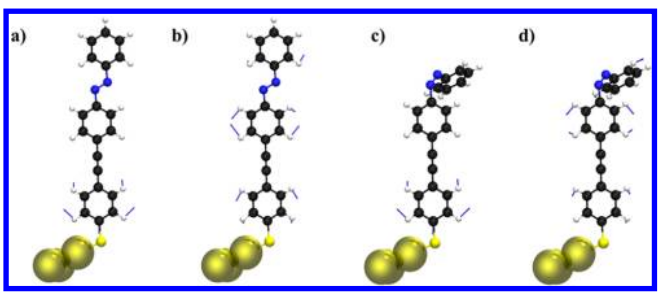

Figure 3. Schematics of the vibrational modes of **Azo2** attached to a Au_3 cluster in (a) P1 trans, (b) P2 trans, (c) P1 cis, and (d) P2 cis geometries. The signal contribution to Raman peaks P1 and P2 is due to the tether and benzene ring of the azobenzene moiety, respectively.

P1 mode (that is isolated to the tether) is minimally affected by isomerization, whereas P2 (an azobenzene mode) is significantly affected. Figure 3 shows the schematic of the vibrational modes of **Azo2** that contributes to the intensity of these peaks in the spectra.

We identified and used peaks P1 and P2 for quantification due to their strong signals and relative sensitivity to isomerization. We followed the change in these peak areas as a function of UV illumination time. As can be seen in Figure 4,

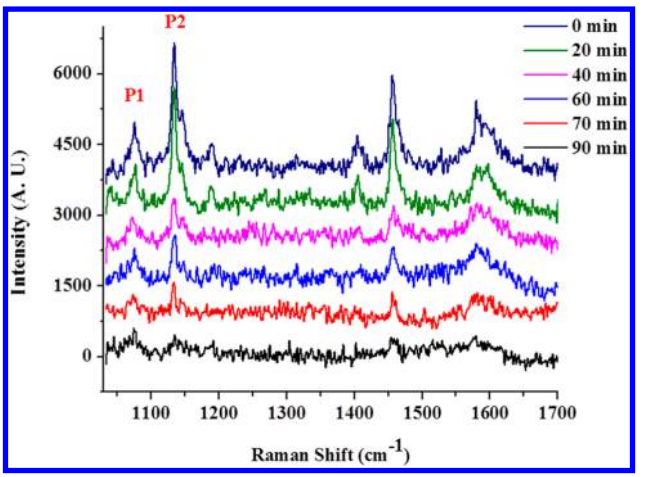

Figure 4. Experimental SERS spectra of **Azo2** on Au{111} nanohole arrays as a function of UV irradiation time (see legend). The spectra have been offset for clarity. The peaks labeled P1 and P2 have been used for monitoring the photoisomerization kinetics.

the peak area of P1 remains relatively unchanged, whereas the peak area of P2 decreases with the duration of UV illumination. The simulated spectra and the experimental results are in close agreement. We chose P1 as an internal standard (due to the minimal effect on its peak area upon photoisomerization), and by comparing the rate of change of the peak area of P2 with respect to P1, a direct measurement of the photoisomerization kinetics of **Azo2** was achieved. We measure the ratio of peak areas of P1 to P2 and plot the change in the ratio as a function of UV illumination.

We measured the peak areas of P1 and P2 from the baseline-subtracted spectra for each data point from 0 to 90 min UV light exposure (~365 nm and power of ~1 mW/cm^2). We then plotted the ratios of peak areas of P1 to P2 versus the duration of UV light exposure. An exponential decay curve was derived by using the formula $Y = Y_0 + A^*e^{(R_0x)}$, where R_0 is the decay constant of the best fit curve, with units of $time^{-1}$. The inverse of the calculated decay constant gave us the time constant τ. We calculated the time constants for both molecules using exactly the same procedure. Figure 5a shows the change in the ratio of peaks P1 to P2 as a function of UV light illumination for the molecule **Azo2**. The plot was generated by taking the average of three data sets (peak area ratios of P1:P2) measured under identical conditions. Figure 5b shows the plot generated from simulated spectra. We have reported the decay plot for **Azo1** previously,[37] wherein we used the peak area ratios of vibrational modes, which were in agreement with the simulated spectra for **Azo1**. The time constant derived from the exponential decay curve of **Azo2** in Figure 5a was found to be $\tau = 61 \pm 11$ min. The time constant from our study with **Azo1** was found to be $\tau = 38 \pm 13$ min (unpublished results).[37]

dx.doi.org/10.1021/jz300968m | J. Phys. Chem. Lett. 2012, 3, 2388−2394

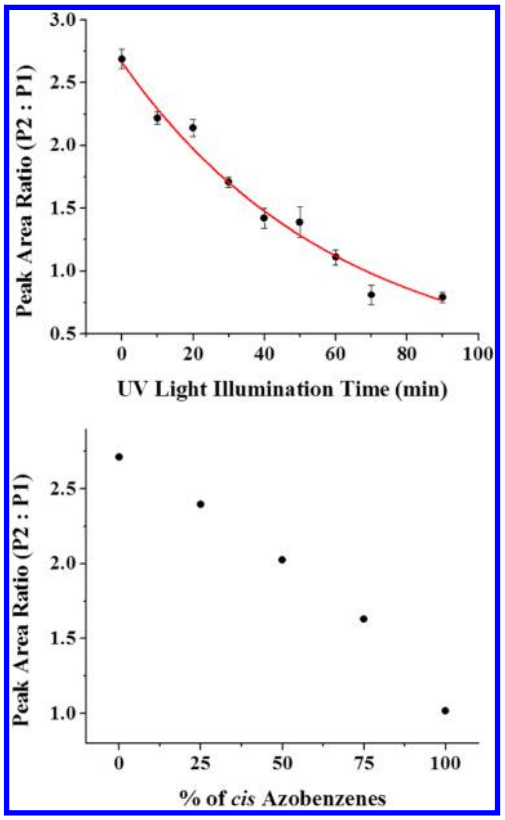

Figure 5. (Top) Experimental decay plot of **Azo2** on Au{111} nanohole array, demonstrating the reduction in the peak area ratio (P2:P1). The calculated time constant from the decay plot was 61 ± 11 min. (Bottom) Decay plot using peak area ratios from simulated SERS spectra showing a decreasing trend.

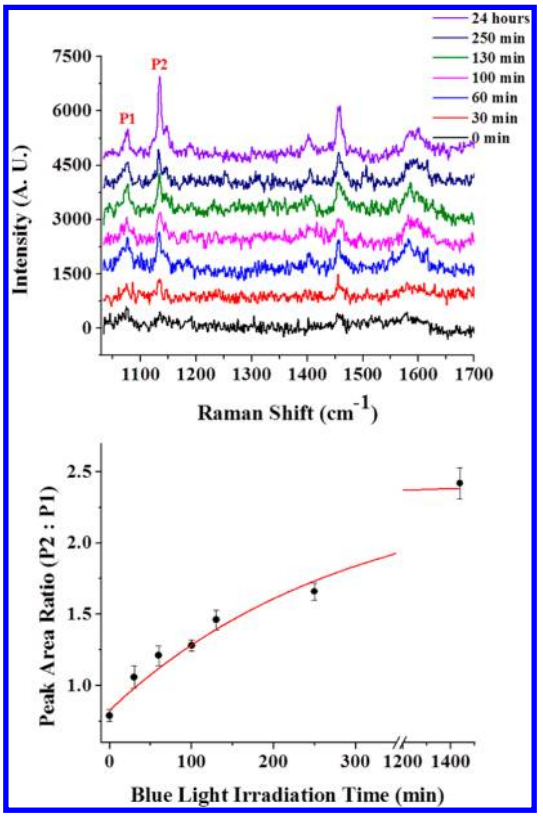

Figure 6. (Top) SERS spectra showing the photoisomerization of **Azo2** back from cis to trans under visible-light illumination over a period of 24 h. (See the legend.) The spectra have been offset for clarity. (Bottom) Exponential curve fit to the ratio of peak areas (P2:P1) shows the slower cis-to-trans back reaction. The *x* axis has been truncated after 250 min to include the 24 h data point. The cis-to-trans photoisomerization of **Azo2** was found to be four times slower when compared with that of **Azo1**.

The reverse isomerization of **Azo2** from cis to trans was also investigated by irradiating the sample with blue light (~450 nm and power of 6 mW/cm^2), whereas **Azo1** showed ~90% reversibility in isomerization within 100 min of visible light illumination,[37] **Azo2** did not exhibit complete reversibility, at least after 24 h of visible light illumination. Figure 6 shows a series of SERS spectra of the surface assembled with **Azo2** under constant visible-light irradiation. (Spectra have been offset for clarity.) Complete reversal in the peak area ratios was not observed after several hours of the time-course study. The samples were then left under visible-light illumination overnight, and spectra were collected after 24 h. It can be seen that the peak areas of P1 and P2 increase dramatically, and the ratio of the peak areas approached the initial ratio before UV illumination. The time constant derived from the experimental curve was found to be 286 ± 37 min (Figure 6) as opposed to the faster cis-to-trans photoisomerization of **Azo1**, which had a time constant of 75 ± 27 min (unpublished results).[37]

Because of the increased conductivity in **Azo2**, the lifetime of the photoexcited state is lower than that in the case of nonconductive tether, resulting in decreased numbers of molecules that undergo photoisomerization over a period of time, resulting in significant difference in the time constants. The experimental studies for both of the molecules were performed under identical conditions, that is, sample preparation, concentration of switch molecules, the nanohole array periodicity of the substrate, power of UV and visible-light sources, and power and beam diameter of the Raman laser source. The only difference was the identity of the tether between the azobenzene functional group and the Au{111} substrate. Because of the ~30° tilt with respect to the surface normal, **Azo1** molecules align themselves in registry with the **C10** molecular tilt, whereas, it has previously been shown that molecules with tethers similar to **Azo2** assemble nominally perpendicular to the underlying Au{111} substrate;[71] we observed similar structures when **Azo2** was assembled on Au{111} (Figure S2 of the Supporting Information). Therefore, even though the lengths of the tethers in **Azo1** and **Azo2** are different, after the assembly on Au{111}, the distances separating the azobenzene moieties in both the molecules from the underlying substrates are nearly the same. Because all of the parameters are left constant other than the identity of the tether, the difference in the time constants can be directly correlated to the change in the conductivity of the tethers. We calculated the photoisomerization cross section of surface-bound **Azo1** and **Azo2** molecules by using the formula $\sigma = hc/(\lambda\tau I_0)$, where h is Planck's constant, c is the speed of light, λ is the wavelength of irradiation (365 nm), τ is the time constant, and I_0 is the power of the UV light source (570 μW/cm^2). By holding all of the experimental parameters constant, we calculate and compare the surface-bound photoisomerization cross section of **Azo1** to be $\sigma_1 = 4.5\ (\pm 1.5) \times 10^{-19}$ cm^2 and of **Azo2** to be $\sigma_2 = 2.5\ (\pm 0.5) \times 10^{-19}$ cm^2. These figures of merit indicate an order of magnitude reduction in cross section of surface-bound molecules when compared with the values in solution.[52] Moreover, the cis-trans isomerization cross section

dx.doi.org/10.1021/jz300968m | J. Phys. Chem. Lett. 2012, 3, 2388−2394

of nonconductive-tethered molecules is an order of magnitude larger than that of conductive-tethered molecules indicating the direct effect of tether conductivity on the photoisomerization of surface-bound molecules. Because it is critical to be able to tune the functionality of surface-bound molecular switches to build efficient functional devices, this letter describes the means to gain that ability by tuning the metal−molecule junction properties and to tailor the efficiency of photoisomerization.

To summarize, we have designed a new conductive tether and demonstrated its effect on the efficiency of photoisomerization of azobenzenes when assembled in precisely controlled nanoscale environments. We have employed SERS to monitor the photoisomerization kinetics of isolated single molecules in well-defined nanoscale environments. By directly comparing the time constants of nonconductive and conductive tethers, we have demonstrated that even when the azobenzene functional moiety is well-separated from the substrate, the efficiency of photoisomerization decreases with increasing conductivity of the tether. This study helps elucidate how to tune the photoswitching efficiency of photochromic molecules for assembly and incorporation into nanoscale assemblies for actuation on the nanoscale.[11]

■ ASSOCIATED CONTENT

Ⓢ Supporting Information

Vibrational modes of prominent peaks of **Azo2** attached to a Au_3 cluster and STM images of **Azo2** assembled on Au{111}. This material is available free of charge via the Internet at http://pubs.acs.org.

■ AUTHOR INFORMATION

Corresponding Author

*E-mail: yangy@ucla.edu (Y.Y.); jensen@chem.psu.edu (L.J.); psw@cnsi.ucla.edu (P.S.W.).

Notes

The authors declare no competing financial interest.

■ ACKNOWLEDGMENTS

We thank the Department of Energy (grant no. DE-FG02-07ER15877), L.J. acknowledges the CAREER program of the National Science Foundation (grant no. CHE-0955689) for financial support, the Penn State Center for Nanoscale Science (a NSF-supported Materials Research Science and Engineering Center), and the Kavli Foundation for support of the work described here. We thank N. Bodzin at UCLA for assistance with FIB lithography.

■ REFERENCES

(1) Amabilino, D. B.; Stoddart, J. F. Interlocked and Intertwined Structures and Superstructures. *Chem. Rev.* **1995**, *95*, 2725−2828.
(2) Balzani, V.; Credi, A.; Raymo, F. M.; Stoddart, J. F. Artificial Molecular Machines. *Angew. Chem., Int. Ed.* **2000**, *39*, 3349−3391.
(3) Feringa, B. L.; van Delden, R. A.; Koumura, N.; Geertsema, E. M. Chiroptical Molecular Switches. *Chem. Rev.* **2000**, *100*, 1789−1816.
(4) Weiss, P. S. Nanotechnology - Molecules Join the Assembly Line. *Nature* **2001**, *413*, 585−586.
(5) Flood, A. H.; Stoddart, J. F.; Steuerman, D. W.; Heath, J. R. Whence Molecular Electronics? *Science* **2004**, *306*, 2055−2056.
(6) Barth, J. V.; Costantini, G.; Kern, K. Engineering Atomic and Molecular Nanostructures at Surfaces. *Nature* **2005**, *437*, 671−679.
(7) Browne, W. R.; Feringa, B. L. Making Molecular Machines Work. *Nature Nanotechnol.* **2006**, *1*, 25−35.
(8) Katsonis, N.; Lubomska, M.; Pollard, M. M.; Feringa, B. L.; Rudolf, P. Synthetic Light-Activated Molecular Switches and Motors on Surfaces. *Prog. Surf. Sci.* **2007**, *82*, 407−434.
(9) Kronemeijer, A. J.; Akkerman, H. B.; Kudernac, T.; van Wees, B. J.; Feringa, B. L.; Blom, P. W. M.; de Boer, B. Reversible Conductance Switching in Molecular Devices. *Adv. Mater.* **2008**, *20*, 1467−1473.
(10) Weiss, P. S. Functional Molecules and Assemblies in Controlled Environments: Formation and Measurements. *Acc. Chem. Res.* **2008**, *41*, 1772−1781.
(11) Li, D.; Paxton, W. F.; Baughman, R. H.; Huang, T. J.; Stoddart, J. F.; Weiss, P. S. Molecular, Supramolecular, and Macromolecular Motors and Artificial Muscles. *MRS Bull.* **2009**, *34*, 671−681.
(12) Kudernac, T.; Ruangsupapichat, N.; Parschau, M.; Macia, B.; Katsonis, N.; Harutyunyan, S. R.; Ernst, K.-H.; Feringa, B. L. Electrically Driven Directional Motion of a Four-Wheeled Molecule on a Metal Surface. *Nature* **2011**, *479*, 208−211.
(13) Weiss, P. S. Nanotechnology: A Molecular Four-Wheel Drive. *Nature* **2011**, *479*, 187−188.
(14) Zheng, Y. B.; Pathem, B. K.; Hohman, J. N.; Thomas, J. C.; Kim, M.; Weiss, P. S. Photoresponsive Molecules in Well-Defined Nanoscale Environments. *Adv. Mater.* **2012**, *24*, in press. DOI: 10.1002/adma.201201532.
(15) Evans, S. D.; Johnson, S. R.; Ringsdorf, H.; Williams, L. M.; Wolf, H. Photoswitching of Azobenzene Derivatives Formed on Planar and Colloidal Gold Surfaces. *Langmuir* **1998**, *14*, 6436−6440.
(16) Zhang, C.; Du, M. H.; Cheng, H. P.; Zhang, X. G.; Roitberg, A. E.; Krause, J. L. Coherent Electron Transport through an Azobenzene Molecule: A Light-Driven Molecular Switch. *Phys. Rev. Lett.* **2004**, *92*, 158301.
(17) Choi, B. Y.; Kahng, S. J.; Kim, S.; Kim, H.; Kim, H. W.; Song, Y. J.; Ihm, J.; Kuk, Y. Conformational Molecular Switch of the Azobenzene Molecule: A Scanning Tunneling Microscopy Study. *Phys. Rev. Lett.* **2006**, *96*, 156106.
(18) Alemani, M.; Peters, M. V.; Hecht, S.; Rieder, K. H.; Moresco, F.; Grill, L. Electric Field-Induced Isomerization of Azobenzene by STM. *J. Am. Chem. Soc.* **2006**, *128*, 14446−14447.
(19) Henzl, J.; Mehlhorn, M.; Gawronski, H.; Rieder, K. H.; Morgenstern, K. Reversible Cis-Trans Isomerization of a Single Azobenzene Molecule. *Angew. Chem., Int. Ed.* **2006**, *45*, 603−606.
(20) Comstock, M. J.; Levy, N.; Kirakosian, A.; Cho, J. W.; Lauterwasser, F.; Harvey, J. H.; Strubbe, D. A.; Frechet, J. M. J.; Trauner, D.; Louie, S. G.; Crommie, M. F. Reversible Photomechanical Switching of Individual Engineered Molecules at a Metallic Surface. *Phys. Rev. Lett.* **2007**, *99*, 038301.
(21) Henningsen, N.; Rurali, R.; Franke, K. J.; Fernandez-Torrente, I.; Pascual, J. I. Trans to Cis Isomerization of an Azobenzene Derivative on a Cu(100) Surface. *Appl. Phys. A: Mater. Sci. Process.* **2008**, *93*, 241−246.
(22) Kumar, A. S.; Ye, T.; Takami, T.; Yu, B. C.; Flatt, A. K.; Tour, J. M.; Weiss, P. S. Reversible Photo-Switching of Single Azobenzene Molecules in Controlled Nanoscale Environments. *Nano Lett.* **2008**, *8*, 1644−1648.
(23) Zarwell, S.; Rueck-Braun, K. Synthesis of an Azobenzene-Linker-Conjugate with Tetrahedrical Shape. *Tetrahedron Lett.* **2008**, *49*, 4020−4025.
(24) Cho, J.; Berbil-Bautista, L.; Levy, N.; Poulsen, D.; Frechet, J. M. J.; Crommie, M. F. Functionalization, Self-Assembly, and Photoswitching Quenching for Azobenzene Derivatives Adsorbed on Au(111). *J. Chem. Phys.* **2010**, *133*, 234707.
(25) Gilat, S. L.; Kawai, S. H.; Lehn, J. M. Light-Triggered Molecular Devices - Photochemical Switching of Optical and Electrochemical Properties in Molecular Wire Type Diarylethene Species. *Chem.—Eur. J* **1995**, *1*, 275−284.
(26) Tian, H.; Yang, S. J. Recent Progresses on Diarylethene Based Photochromic Switches. *Chem. Soc. Rev.* **2004**, *33*, 85−97.
(27) Kobatake, S.; Takami, S.; Muto, H.; Ishikawa, T.; Irie, M. Rapid and Reversible Shape Changes of Molecular Crystals on Photoirradiation. *Nature* **2007**, *446*, 778−781.

(28) Raymo, F. M.; Alvarado, R. J.; Giordani, S.; Cejas, M. A. Memory Effects Based on Intermolecular Photoinduced Proton Transfer. *J. Am. Chem. Soc.* **2003**, *125*, 2361−2364.
(29) Raymo, F. M.; Giordani, S.; White, A. J. P.; Williams, D. J. Digital Processing with a Three-State Molecular Switch. *J. Org. Chem.* **2003**, *68*, 4158−4169.
(30) Zheng, Y. B.; Kiraly, B.; Cheunkar, S.; Huang, T. J.; Weiss, P. S. Incident-Angle-Modulated Molecular Plasmonic Switches: A Case of Weak Exciton-Plasmon Coupling. *Nano Lett.* **2011**, *11*, 2061−2065.
(31) Gobbi, L.; Seiler, P.; Diederich, F.; Gramlich, V.; Boudon, C.; Gisselbrecht, J. P.; Gross, M. Photoswitchable Tetraethynylethene-Dihydroazulene Chromophores. *Helv. Chim. Acta* **2001**, *84*, 743−777.
(32) Boggio-Pasqua, M.; Bearpark, M. J.; Hunt, P. A.; Robb, M. A. Dihydroazulene/Vinylheptafulvene Photochromism: A Model for One-Way Photochemistry via a Conical Intersection. *J. Am. Chem. Soc.* **2002**, *124*, 1456−1470.
(33) Broman, S. L.; Petersen, M. A.; Tortzen, C. G.; Kadziola, A.; Kilsa, K.; Nielsen, M. B. Arylethynyl Derivatives of the Dihydroazulene/Vinylheptafulvene Photo/Thermoswitch: Tuning the Switching Event. *J. Am. Chem. Soc.* **2010**, *132*, 9165−9174.
(34) Parker, C. R.; Tortzen, C. G.; Broman, S. L.; Schau-Magnussen, M.; Kilsa, K.; Nielsen, M. B. Lewis Acid Enhanced Switching of the 1,1-Dicyanodihydroazulene/vinylheptafulvene Photo/Thermoswitch. *Chem. Commun.* **2011**, *47*, 6102−6104.
(35) Tsuji, T.; Takeuchi, H.; Egawa, T.; Konaka, S. Effects of Molecular Structure on the Stability of a Thermotropic Liquid Crystal. Gas Electron Diffraction Study of the Molecular Structure of Phenyl Benzoate. *J. Am. Chem. Soc.* **2001**, *123*, 6381−6387.
(36) Fliegl, H.; Kohn, A.; Hattig, C.; Ahlrichs, R. Ab Initio Calculation of the Vibrational and Electronic Spectra of trans- and cis-Azobenzene. *J. Am. Chem. Soc.* **2003**, *125*, 9821−9827.
(37) Zheng, Y. B.; Payton, J. L.; Chung, C.-H.; Liu, R.; Cheunkar, S.; Pathem, B. K.; Yang, Y.; Jensen, L.; Weiss, P. S. Surface-Enhanced Raman Spectroscopy to Probe Reversibly Photoswitchable Azobenzene in Controlled Nanoscale Environments. *Nano Lett.* **2011**, *11*, 3447−3452.
(38) Comstock, M. J.; Strubbe, D. A.; Berbil-Bautista, L.; Levy, N.; Cho, J.; Poulsen, D.; Frechet, J. M. J.; Louie, S. G.; Crommie, M. F. Determination of Photoswitching Dynamics through Chiral Mapping of Single Molecules Using a Scanning Tunneling Microscope. *Phys. Rev. Lett.* **2010**, *104*, 178301.
(39) Pechenezhskiy, I. V.; Cho, J.; Nguyen, G. D.; Berbil-Bautista, L.; Giles, B. L.; Poulsen, D. A.; Frechet, J. M. J.; Crommie, M. F. Self-Assembly and Photomechanical Switching of an Azobenzene Derivative on GaAs(110): Scanning Tunneling Microscopy Study. *J. Phys. Chem. C* **2012**, *116*, 1052−1055.
(40) Henzl, J.; Puschnig, P.; Ambrosch-Draxl, C.; Schaate, A.; Ufer, B.; Behrens, P.; Morgenstern, K. Photoisomerization for a Molecular Switch in Contact with a Surface. *Phys. Rev. B* **2012**, *85*, 035410.
(41) Zheng, Y. B.; Kiraly, B.; Weiss, P. S.; Huang, T. J. Molecular Plasmonics for Biology and Nanomedicine. *Nanomedicine* **2012**, *7*, 751−770.
(42) Lewis, P. A.; Inman, C. E.; Yao, Y. X.; Tour, J. M.; Hutchison, J. E.; Weiss, P. S. Mediating Stochastic Switching of Single Molecules Using Chemical Functionality. *J. Am. Chem. Soc.* **2004**, *126*, 12214−12215.
(43) Moore, A. M.; Mantooth, B. A.; Donhauser, Z. J.; Maya, F.; Price, D. W.; Yao, Y. X.; Tour, J. M.; Weiss, P. S. Cross-Step Place-Exchange of Oligo(Phenylene-Ethynylene) Molecules. *Nano Lett.* **2005**, *5*, 2292−2297.
(44) Willner, I.; Rubin, S. Control of the Structure and Functions of Biomaterials by Light. *Angew. Chem., Int. Ed.* **1996**, *35*, 367−385.
(45) Riskin, M.; Willner, I. Coupled Electrochemical/Photochemical Patterning and Erasure of Ag^0 Nanoclusters on Au Surfaces. *Langmuir* **2009**, *25*, 13900−13905.
(46) Alemani, M.; Selvanathan, S.; Ample, F.; Peters, M. V.; Rieder, K.-H.; Moresco, F.; Joachim, C.; Hecht, S.; Grill, L. Adsorption and Switching Properties of Azobenzene Derivatives on Different Noble Metal Surfaces: Au(111), Cu(111), and Au(100). *J. Phys. Chem. C* **2008**, *112*, 10509−10514.
(47) Jung, U.; Filinova, O.; Kuhn, S.; Zargarani, D.; Bornholdt, C.; Herges, R.; Magnussen, O. Photoswitching Behavior of Azobenzene-Containing Alkanethiol Self-Assembled Monolayers on Au Surfaces. *Langmuir* **2010**, *26*, 13913−13923.
(48) Xu, S.; Shan, J.; Shi, W.; Liu, L.; Xu, L. Modifying Photoisomerization Efficiency by Metallic Nanostructures. *Opt. Express* **2011**, *19*, 12336−12341.
(49) Shipway, A. N.; Katz, E.; Willner, I. Nanoparticle Arrays on Surfaces for Electronic, Optical, and Sensor Applications. *ChemPhysChem* **2000**, *1*, 18−52.
(50) Stavytska-Barba, M.; Salvador, M.; Kulkarni, A.; Ginger, D. S.; Kelley, A. M. Plasmonic Enhancement of Raman Scattering from the Organic Solar Cell Material P3HT/PCBM by Triangular Silver Nanoprisms. *J. Phys. Chem. C* **2011**, *115*, 20788−20794.
(51) Qune, L. F. N. A.; Akiyama, H.; Nagahiro, T.; Tamada, K.; Wee, A. T. S. Reversible Work Function Changes Induced by Photoisomerization of Asymmetric Azobenzene Dithiol Self-Assembled Monolayers on Gold. *Appl. Phys. Lett.* **2008**, *93*, 083109.
(52) Wagner, S.; Leyssner, F.; Koerdel, C.; Zarwell, S.; Schmidt, R.; Weinelt, M.; Rueck-Braun, K.; Wolf, M.; Tegeder, P. Reversible Photoisomerization of an Azobenzene-Functionalized Self-Assembled Monolayer Probed by Sum-Frequency Generation Vibrational Spectroscopy. *Phys. Chem. Chem. Phys.* **2009**, *11*, 6242−6248.
(53) Ye, T.; Kumar, A. S.; Saha, S.; Takami, T.; Huang, T. J.; Stoddart, J. F.; Weiss, P. S. Changing Stations in Single Bistable Rotaxane Molecules under Electrochemical Control. *ACS Nano* **2010**, *4*, 3697−3701.
(54) Moore, A. M.; Yeganeh, S.; Yao, Y.; Claridge, S. A.; Tour, J. M.; Ratner, M. A.; Weiss, P. S. Polarizabilities of Adsorbed and Assembled Molecules: Measuring the Conductance through Buried Contacts. *ACS Nano* **2010**, *4*, 7630−7636.
(55) Joachim, C. The Conductance of a Single Molecule. *New J. Chem.* **1991**, *15*, 223−229.
(56) Bumm, L. A.; Arnold, J. J.; Cygan, M. T.; Dunbar, T. D.; Burgin, T. P.; Jones, L.; Allara, D. L.; Tour, J. M.; Weiss, P. S. Are Single Molecular Wires Conducting? *Science* **1996**, *271*, 1705−1707.
(57) Bumm, L. A.; Arnold, J. J.; Dunbar, T. D.; Allara, D. L.; Weiss, P. S. Electron Transfer through Organic Molecules. *J. Phys. Chem. B* **1999**, *103*, 8122−8127.
(58) Holmlin, R. E.; Ismagilov, R. F.; Haag, R.; Mujica, V.; Ratner, M. A.; Rampi, M. A.; Whitesides, G. M. Correlating Electron Transport and Molecular Structure in Organic Thin Films. *Angew. Chem., Int. Ed.* **2001**, *40*, 2316−2320.
(59) Beebe, J. M.; Engelkes, V. B.; Miller, L. L.; Frisbie, C. D. Contact Resistance in Metal−Molecule−Metal Junctions Based on Aliphatic SAMs: Effects of Surface Linker and Metal Work Function. *J. Am. Chem. Soc.* **2002**, *124*, 11268−11269.
(60) Salomon, A.; Cahen, D.; Lindsay, S.; Tomfohr, J.; Engelkes, V. B.; Frisbie, C. D. Comparison of Electronic Transport Measurements on Organic Molecules. *Adv. Mater.* **2003**, *15*, 1881−1890.
(61) Engelkes, V. B.; Beebe, J. M.; Frisbie, C. D. Length-Dependent Transport in Molecular Junctions Based on SAMs of Alkanethiols and Alkanedithiols: Effect of Metal Work Function and Applied Bias on Tunneling Efficiency and Contact Resistance. *J. Am. Chem. Soc.* **2004**, *126*, 14287−14296.
(62) Monnell, J. D.; Stapleton, J. J.; Dirk, S. M.; Reinerth, W. A.; Tour, J. M.; Allara, D. L.; Weiss, P. S. Relative Conductances of Alkaneselenolate and Alkanethiolate Monolayers on Au{111}. *J. Phys. Chem. B* **2005**, *109*, 20343−20349.
(63) Kim, B.; Choi, S. H.; Zhu, X. Y.; Frisbie, C. D. Molecular Tunnel Junctions Based on π-Conjugated Oligoacene Thiols and Dithiols between Ag, Au, and Pt Contacts: Effect of Surface Linking Group and Metal Work Function. *J. Am. Chem. Soc.* **2011**, *133*, 19864−19877.
(64) Sachs, S. B.; Dudek, S. P.; Hsung, R. P.; Sita, L. R.; Smalley, J. F.; Newton, M. D.; Feldberg, S. W.; Chidsey, C. E. D. Rates of Interfacial Electron Transfer through π-Conjugated Spacers. *J. Am. Chem. Soc.* **1997**, *119*, 10563−10564.

(65) Donhauser, Z. J.; Mantooth, B. A.; Kelly, K. F.; Bumm, L. A.; Monnell, J. D.; Stapleton, J. J.; Price, D. W.; Rawlett, A. M.; Allara, D. L.; Tour, J. M.; Weiss, P. S. Conductance Switching in Single Molecules through Conformational Changes. *Science* **2001**, *292*, 2303−2307.
(66) Kushmerick, J. G.; Holt, D. B.; Pollack, S. K.; Ratner, M. A.; Yang, J. C.; Schull, T. L.; Naciri, J.; Moore, M. H.; Shashidhar, R. Effect of Bond-Length Alternation in Molecular Wires. *J. Am. Chem. Soc.* **2002**, *124*, 10654−10655.
(67) Donhauser, Z. J.; Price, D. W.; Tour, J. M.; Weiss, P. S. Control of Alkanethiolate Monolayer Structure Using Vapor-Phase Annealing. *J. Am. Chem. Soc.* **2003**, *125*, 11462−11463.
(68) Stranick, S. J.; Parikh, A. N.; Allara, D. L.; Weiss, P. S. A New Mechanism for Surface Diffusion: Motion of a Substrate-Adsorbate Complex. *J. Phys. Chem.* **1994**, *98*, 11136−11142.
(69) Bumm, L. A.; Arnold, J. J.; Charles, L. F.; Dunbar, T. D.; Allara, D. L.; Weiss, P. S. Directed Self-Assembly to Create Molecular Terraces with Molecularly Sharp Boundaries in Organic Monolayers. *J. Am. Chem. Soc.* **1999**, *121*, 8017−8021.
(70) Valiev, M.; Bylaska, E. J.; Govind, N.; Kowalski, K.; Straatsma, T. P.; van Dam, H. J. J.; Wang, D.; Nieplocha, J.; Apra, E.; Windus, T. L.; de Jong, W. A. NWChem: A Comprehensive and Scalable Open-Source Solution for Large Scale Molecular Simulations. *Comput. Phys. Commun.* **2010**, *181*, 1477.
(71) Yang, G. H.; Qian, Y. L.; Engtrakul, C.; Sita, L. R.; Liu, G. Y. Arenethiols Form Ordered and Incommensurate Self-Assembled Monolayers on Au(111) Surfaces. *J. Phys. Chem. B* **2000**, *104*, 9059−9062.